An Updated Comprehensive Kinetic Model of Hydrogen Combustion

JUAN LI, ZHENWEI ZHAO, ANDREI KAZAKOV, FREDERICK L. DRYER

Department of Mechanical and Aerospace Engineering, Princeton University, Princeton, NJ 08544-5263

Received 8 January 2004; revised 2 May 2004; accepted 11 May 2004

DOI 10.1002/kin.20026
Published online in Wiley InterScience (www.interscience.wiley.com).

ABSTRACT: A comprehensively tested H_2/O_2 chemical kinetic mechanism based on the work of Mueller et al. [1] and recently published kinetic and thermodynamic information is presented. The revised mechanism is validated against a wide range of experimental conditions, including those found in shock tubes, flow reactors, and laminar premixed flame. Excellent agreement of the model predictions with the experimental observations demonstrates that the mechanism is comprehensive and has good predictive capabilities for different experimental systems, including new results published subsequent to the work of Mueller et al. [1], particularly high-pressure laminar flame speed and shock tube ignition results. The reaction $H + OH + M$ is found to be primarily significant only to laminar flame speed propagation predictions at high pressure. All experimental hydrogen flame speed observations can be adequately fit using any of the several transport coefficient estimates presently available in the literature for the hydrogen/oxygen system simply by adjusting the rate parameters for this reaction within their present uncertainties.
 Int J Chem Kinet 36: 566–575, 2004

INTRODUCTION

The H_2/O_2 reaction mechanism plays a prominent role in fundamental chemical kinetics research as well as in the applied fields of fire safety, energy conversion, and propulsion. Not only is hydrogen an important fuel for these applications, but the elementary kinetics involving H, O, OH, HO_2, and H_2O_2 determine the composition of the radical pool in hydrocarbon reaction systems. The reaction system and associated mechanistic representations have been used extensively by several research groups including ours in various experiments to derive elementary reaction rate information, for example, by perturbations of kinetics using added species. The kinetics of the H_2/O_2 system and its behavior over a range of experiments conducted in a variable pressure flow reactor (VPFR) were recently discussed by Mueller et al. [1]. The initial mechanism development relied heavily on the earlier work of Yetter et al. [2] on the moist carbon monoxide oxidation system, which was comprehensively studied. The mechanism presented in Ref. [1] was extensively studied at flow reactor conditions, but it was not tested against or modified as a result of comparisons with experimental data derived in other types of experiments and in other parameter ranges. Indeed, the authors noted several issues that deserved further attention in applying the mechanism more generally. In the strictest sense,

Parts of this work were initially presented at the Fall Eastern States Section Technical Meeting of the Combustion Institute, Pennsylvania State University, University Park, PA, October 26–29, 2003.

Correspondence to: Frederick L. Dryer; e-mail: fldryer@princeton.edu.

Contract grant sponsor: Division of Chemical Sciences, Geosciences, and Biosciences, Office of Basic Energy Sciences, Office of Science, U.S. Department of Energy.

Contract grant number: DE-FG02-86ER13503.

the published mechanism was therefore not *comprehensive*, a term originally applied by Westbrook and Dryer [3,4] to describe a mechanism developed by comparison against a number of different sources of kinetic data. These sources frequently include laminar flame speed measurements [5–8], shock tube ignition delay studies [9–14], and other sources such as static and stirred reactors. New flame speed experimental results using H_2/O_2/He mixtures at pressures ranging from 1 to 20 atm appear to be poorly predicted by the Mueller et al. mechanism [7], while predictions of similar experiments using H_2/O_2 mixtures in argon, helium, and nitrogen at 1–3 atm pressure are quite reasonable [8]. Recently, Curran and coworkers [15] have made wide-ranging comparisons with various experimental data and they have in addition noted that the mechanism in Ref. [1] substantially overpredicts shock tube ignition delay data reported by Skinner et al. [11].

Since the publication of Ref. [1], there have been several important elementary kinetic publications further addressing two of the most important reactions involving the hydrogen radical, i.e., the branching reaction [16],

$$H + O_2 = OH + O \qquad (R1)$$

and the competitive reaction [17–20],

$$H + O_2(+M) = HO_2(+M) \qquad (R2)$$

While some of the results presented in Ref. [19] were known at the time of our earlier consideration of reaction (R2) [21], Ref. [19] contributes new insights to the magnitudes of and the mechanism responsible for the apparent third-body efficiencies of various species in reaction (R2), particularly H_2O. In addition, the enthalpy of formation of OH has recently been conclusively revised [22].

In the present study, we update the mechanism of Ref. [1] based upon the new thermodynamic data and rate coefficients, and compare the updated mechanism against a wide array of experimental data including the original VPFR data, shock tube ignition delay data, and the new flame speed results to yield a "comprehensive" hydrogen oxygen mechanism.

We wish to emphasize, however, that the term *comprehensive* carries no inference as to whether a mechanism is "complete," "unique," and will never require further revisions. Additional experimental systems observations that increase the constraints defining the acceptability of predictive comparisons and/or improvements in uncertainties of elementary kinetic information (rate data, thermochemistry) can both inspire the need to revise a previously developed comprehensive mechanism. Thus, even comprehensive mechanisms should be reviewed in a timely manner as new information becomes available. This is a perplexing, but extremely important issue in light of the hierarchical nature of hydrocarbon kinetics and its dependence on H_2/O_2 kinetics. Revisions of mechanisms are likely to be necessary in perpetuity, given the nature of the field. Moreover, even the most complete mechanistic description to be envisioned will most likely never be unique in terms of the associated elementary reaction rate and thermochemical parameters.

Updated H_2/O_2 Chemical Kinetics

The updated detailed H_2/O_2 reaction mechanism consists of 19 reversible elementary reactions and thermochemical data listed in Tables I and II, respectively. Reverse rate constants are computed from the forward rate constants and the equilibrium constants. The third-body efficiency of helium is assumed to be the same as that of argon, except for reaction (9) in Table I. In the present work, the following parameters of mechanism presented in Mueller et al. [1] are revised.

The Enthalpy of Formation of OH. Recently, Ruscic et al. [22] studied the heat of formation of OH radical both experimentally and theoretically, and the recommended value of 8.91 kcal/mol at 298 K is in excellent agreement with the recent experimental result of 8.92 kcal/mol [23]. The heat of formation value presented by Ruscic et al. [22] is used in the current mechanism.

The Rate Constant of Reaction (R1). We performed a sensitivity analysis of the original mechanism for a VPFR case at 3.4 atm [1], for a premixed laminar flame speed at 10 atm [7], and for an ignition delay case under Skinner et al. [11] shock tube conditions. The normalized sensitivity coefficient of a reaction is defined as $\frac{\partial \ln Y}{\partial \ln k}$, $\frac{\partial \ln s}{\partial \ln k}$, and $\frac{\partial \ln \tau}{\partial \ln k}$ for the disappearance of a species Y in a flow reactor, for the laminar flame speed, and for ignition delay time, respectively, where k is the rate constant, Y the mass fraction of a species (H_2 in this study), s the laminar flame speed, and τ the ignition delay time. The most sensitive reactions found are shown in Fig. 1 along with their sensitivity coefficients as defined above.

As is well known through the literature and also shown in Fig. 1, the H_2/O_2 system is very sensitive to the key chain-branching reaction (R1) and the important chain-termination reaction (R2). Mueller et al. [1] used the rate constant expression of Pirraglia et al. [24] for the reaction (R1) and noted that while the expression overpredicts the recent high temperature data above

Table I Detailed H_2/O_2 Reaction Mechanism

		A	n	E	Reference
H_2/O_2 chain reactions					
1. $H + O_2 = O + OH$		3.55×10^{15}	−0.41	16.6	[16]
2. $O + H_2 = H + OH$		5.08×10^{4}	2.67	6.29	[44]
3. $H_2 + OH = H_2O + H$		2.16×10^{8}	1.51	3.43	[45]
4. $O + H_2O = OH + OH$		2.97×10^{6}	2.02	13.4	[46]
H_2/O_2 dissociation/recombination reactions					
5. $H_2 + M = H + H + M^a$		4.58×10^{19}	−1.40	104.38	[47]
$H_2 + Ar = H + H + Ar$		5.84×10^{18}	−1.10	104.38	[47]
$H_2 + He = H + H + He$		5.84×10^{18}	−1.10	104.38	See text
6. $O + O + M = O_2 + M^a$		6.16×10^{15}	−0.50	0.00	[47]
$O + O + Ar = O_2 + Ar$		1.89×10^{13}	0.00	−1.79	[47]
$O + O + He = O_2 + He$		1.89×10^{13}	0.00	−1.79	See text
7. $O + H + M = OH + M^a$		4.71×10^{18}	−1.0	0.00	[47]
8. $H + OH + M = H_2O + M^b$		3.8×10^{22}	−2.00	0.00	See text
Formation and consumption of HO_2					
9. $H + O_2 + M = HO_2 + M^c$	k_0	6.37×10^{20}	−1.72	0.52	[19]
$H + O_2 + M = HO_2 + M^d$	k_0	9.04×10^{19}	−1.50	0.49	[19]
	k_∞	1.48×10^{12}	0.60	0.00	[48]
10. $HO_2 + H = H_2 + O_2$		1.66×10^{13}	0.00	0.82	[1]
11. $HO_2 + H = OH + OH$		7.08×10^{13}	0.00	0.30	[1]
12. $HO_2 + O = OH + O_2$		3.25×10^{13}	0.00	0.00	[34]
13. $HO_2 + OH = H_2O + O_2$		2.89×10^{13}	0.00	−0.50	[34]
Formation and consumption of H_2O_2					
14. $HO_2 + HO_2 = H_2O_2 + O_2^e$		4.20×10^{14}	0.00	11.98	[49]
$HO_2 + HO_2 = H_2O_2 + O_2$		1.30×10^{11}	0.00	−1.63	
15. $H_2O_2 + M = OH + OH + M^f$	k_0	1.20×10^{17}	0.00	45.5	[50]
	k_∞	2.95×10^{14}	0.00	48.4	[51]
16. $H_2O_2 + H = H_2O + OH$		2.41×10^{13}	0.00	3.97	[47]
17. $H_2O_2 + H = H_2 + HO_2$		4.82×10^{13}	0.00	7.95	[47]
18. $H_2O_2 + O = OH + HO_2$		9.55×10^{6}	2.00	3.97	[47]
19. $H_2O_2 + OH = H_2O + HO_2^e$		1.00×10^{12}	0.00	0.00	[52]
$H_2O_2 + OH = H_2O + HO_2$		5.8×10^{14}	0.00	9.56	

Units are cm^3-mol-s-kcal-K, and $k = AT^n \exp(-E/RT)$

[a] Efficiency factors are: $\varepsilon_{H_2O} = 12.0$, $\varepsilon_{H_2} = 2.5$, $\varepsilon_{Ar} = 0.75$, and $\varepsilon_{He} = 0.75$. When a rate constant is declared specifically for Ar or He collision partner, the efficiency of Ar or He is set to zero when determining M for the same reaction.

[b] Efficiency factors are $\varepsilon_{H_2O} = 12.0$, $\varepsilon_{H_2} = 2.5$, $\varepsilon_{Ar} = 0.38$, and $\varepsilon_{He} = 0.38$.

[c] When the main bath gas is N_2 (M = N_2). Troe parameter is $F_c = 0.8$. Efficiency factors are $\varepsilon_{H_2O} = 11.0$, $\varepsilon_{H_2} = 2.0$, and $\varepsilon_{O_2} = 0.78$.

[d] When the main bath gas is Ar or He (M = Ar or He). Troe parameter is $F_c = 0.5$. Efficiency factors are $\varepsilon_{H_2O} = 16.0$, $\varepsilon_{H_2} = 3.0$, $\varepsilon_{O_2} = 1.1$, and $\varepsilon_{He} = 1.2$.

[e] Reactions (14) and (19) are expressed as the sum of the two rate expressions.

[f] Troe parameter is $F_c = 0.5$. Efficiency factors are $\varepsilon_{H_2O} = 12.0$, $\varepsilon_{H_2} = 2.5$, $\varepsilon_{Ar} = 0.64$, and $\varepsilon_{He} = 0.64$.

1700 K [25–27], it more properly predicts the rate at low temperatures. The recent analysis of Hessler [16] excluded consideration of certain sets of available elementary rate data [27] based upon a defined uncertainty envelope. The resulting rate constant correlation predicts not only the data in Refs. [24–26], but also more closely predicts appropriate rates at low temperatures within close proximity to those predicted by the expression in Ref. [24]. In the present mechanism, the rate constant of reaction (R1) is updated to that in Hessler [16]. Figure 2 compares the predictions of the rate constant of reaction (R1) available in the literature. Yu et al. [28] analyzed the shock tube experimental data of Refs. [25] and [29], and used an H_2/O_2 mechanism to derive the rate constant of reaction (R1) over 1336–3370 K. As shown in Fig. 2, over this temperature range, the prediction of Hessler [16] is close to those of Refs. [25] and [28] (within 15%). The reasons driving us to choose the correlation of Hessler [16] over others will become clear below.

Table II ΔH_f (298.15), S (298.15), and C_p (T) for Species Considered in the H_2/O_2 Reaction Mechanism*

Species	ΔH_f (298.15)	S (298.15)	C_p (300)	C_p (500)	C_p (800)	C_p (1000)	C_p (1500)	C_p (2000)
H	52.10	27.39	4.97	4.97	4.97	4.97	4.97	4.97
O	59.56	38.47	5.23	5.08	5.02	5.00	4.98	4.98
OH	8.91	43.91	7.16	7.05	7.15	7.34	7.87	8.28
H_2	0.0	31.21	6.90	7.00	7.07	7.21	7.73	8.18
O_2	0.0	49.01	7.01	7.44	8.07	8.35	8.72	9.03
H_2O	−57.80	45.10	8.00	8.45	9.22	9.87	11.26	12.22
HO_2	3.0	54.76	8.35	9.47	10.77	11.38	12.48	13.32
H_2O_2	−32.53	55.66	10.42	12.35	14.29	15.21	16.85	17.88
N_2	0.0	45.77	6.95	7.08	7.50	7.83	8.32	8.60
Ar	0.0	36.98	4.97	4.97	4.97	4.97	4.97	4.97
He	0.0	30.12	4.97	4.97	4.97	4.97	4.97	4.97

Units are cal/mol/K for S and C_p, and kcal/mol for ΔH_f.

The Low-Pressure-Limit Rate Constant of Reaction (R2). The Troe formulation [30] is applied for reaction (R2) with the high-pressure-limit rate constant used in Ref. [1], and the low-pressure-limit results, $k_{0,}$ reported in [19]. Michael et al. [19] calculated k_0 with M representing N_2, Ar, He, H_2, H_2O, and O_2,and verified calculated values against experimental data. We fitted the data that were presented in the paper for each third-body condition to capture both the rate constant and bath gas temperature dependences. The calculated fits in Arrhenius form for a bath gas of N_2 or Ar are as follows (in units of $cm^6\ mol^{-2}\ s^{-1}$):

$$k_0^{N_2} = 6.37 \times 10^{20} T^{-1.72} \exp(-264/T)$$
$$k_0^{Ar} = 9.04 \times 10^{19} T^{-1.50} \exp(-248/T)$$

The third-body efficiency of He, H_2, O_2, and H_2O are taken as the average value over the temperature range of 300–3000 K. The fall-off range of reaction (R2) is described by taking the broadening factor F_c as 0.8 for N_2, and 0.5 for Ar. This implementation represents a

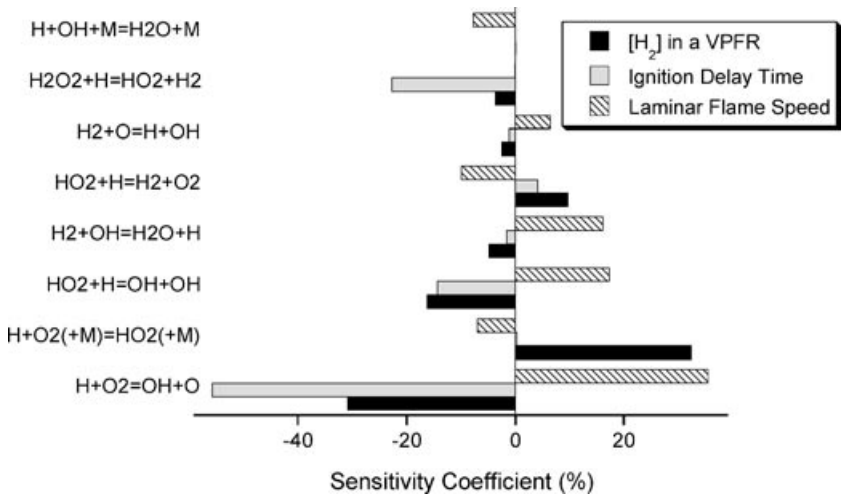

Figure 1 Sensitivity coefficient of reactions for a flow reactor [1], laminar flame speed [7], and shock tube ignition delay [11] case calculated by using the mechanism of Mueller et al. [1]. Initial conditions: $H_2 = 1.01\%$, $O_2 = 0.52\%$ with balance N_2 at 3.4 atm and 933 K [1]; $H_2 = 19.4\%$, $O_2 = 6.5\%$ with balance He at 10 atm and 298 K [7]; $H_2 = 8.0\%$, $O_2 = 2.0\%$ with balance Ar at 5 atm and 960 K [11]. The sensitivity coefficient for the flow reactor case is taken at the time when 50% H_2 has been consumed.

*After acceptance of the present work for publication, we became aware of a new evaluation of the standard heat of formation of HO_2 [54]. The new value is 2.88 ± 0.15 kcal/mol (as opposed to the previous value of 3.0 kcal/mol given in Table II). While all of the results presented here were obtained with an old value, we have confirmed that using this new result [54] does not produce noticeable changes in the model predictions. The new value is therefore recommended for the future use of the present mechanism.

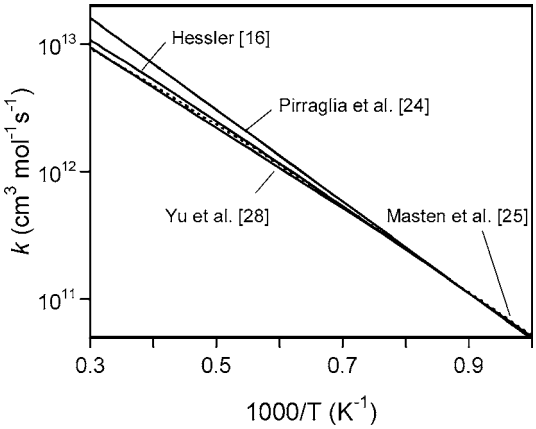

Figure 2 Rate coefficient of reaction $H + O_2 \rightarrow OH + O$.

compromise formulation that responds to (1) the limitations of CHEMKIN-II format, especially, an inability to implement temperature-dependent collision efficiencies in fall-off reactions, and (2) the lack of fundamental understanding of the mixing rules for the fall-off reactions with bath gases having different broadening factors. As a consequence, the fall-off kinetics of reaction (R2) is expressed in two groups, for N_2 and Ar/He as the bath gas, respectively.

The predictions of k_0 of reaction (R2) reported in some recent publications are shown in Fig. 3. As can be seen, the result of Michael et al. [19] is in very good agreement with that of Ref. [18]. Figure 4 shows the temperature and pressure dependence of the rate constant of reaction (R2) predicted by the present mechanism and by Troe [17]. We see that these two predictions agree reasonably well (within 20%) with each other over 300–3000 K and from low- to high-pressure range.

Figure 5 shows the branching ratio, i.e. (R2)/(R1), at 0.1, 1, and 10 atm with the current revisions and from

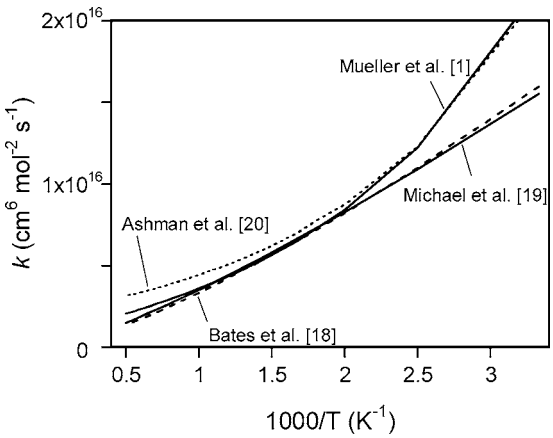

Figure 3 Rate coefficient of reaction $H + O_2 + M \rightarrow HO_2 + M$ for $M = N_2$.

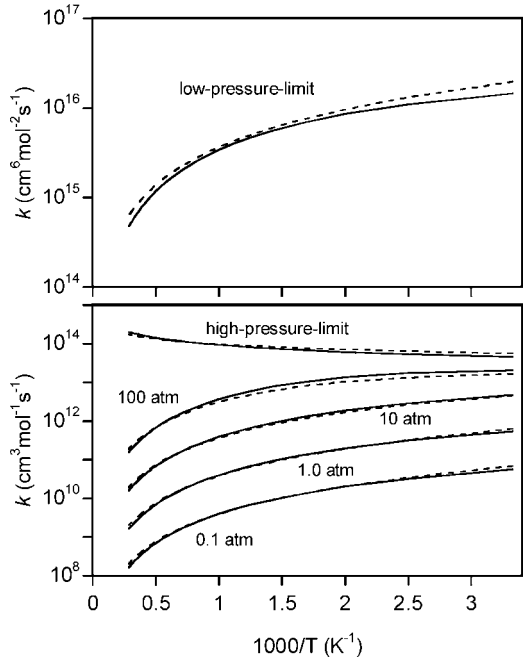

Figure 4 Temperature and pressure dependence of the reaction rate of $H + O_2(+M) \rightarrow HO_2 (+M)$ for $M = N_2$. Solid lines represent the values used in the present mechanism, and dashed lines the recommendations of Ref. [17].

Ref. [1]. There is very good agreement (within 2%) at the conditions (800–900 K) where the value of k_0 used in [1] was experimentally derived [31]. At temperature higher than 2000 K, the difference between the two predictions becomes larger (~30%), but reaction (R2) is of no significance at these conditions relative to reaction (R1). Achieving agreement of this ratio at 800–900 K is very important to this update, as not only is this a temperature region most sensitive to the ratio, but our earlier work [31] defined this ratio experimentally with a very small uncertainty. As mentioned

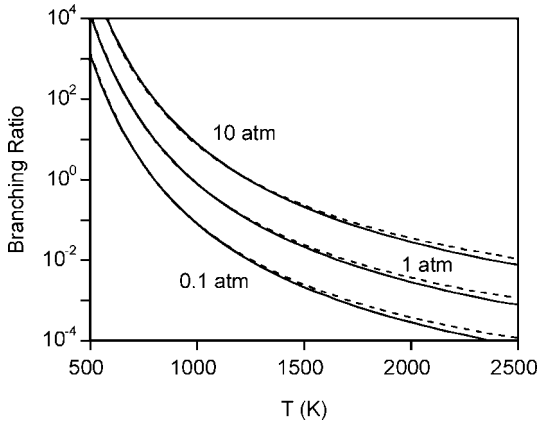

Figure 5 Branching ratio of reactions (R1) and (R2). Solid lines: the present model; dashed lines: the model of Mueller et al. [1].

in Mueller et al. [21], the use of data for reaction (R1) from other sources did not result in the appropriate ratio when combined with their independent measurement of reaction (R2) in this temperature range. The uncertainty in this experimental determination was recently reviewed and further reduced by additional analyses [32]. On the other hand, the determined value of reaction (R2) agrees very well with the extrapolation of the measurements obtained by Michael et al. [19] to flow reactor temperatures.

The Rate Constant of Reaction H + OH + M = H_2O + M. The sensitivity analysis in Fig. 1 also indicates that the laminar flame speed case is sensitive to reaction (R3), while flow reactor and shock tube ignition delay predictions are essentially insensitive to this reaction at all conditions. In order to improve flame predictions, we modified the *A* factor of the rate constant of reaction (R3) to 3.8×10^{22} $cm^6\,mol^{-2}\,s^{-1}$ (from 2.2×10^{22} [1]). Curran and coworkers [15] also suggest modification of this reaction to improve flame speed predictions. Figure 6 shows a review of the rate constant reported in the literature for reaction (R3) [33–39]. Obviously, the rate constant results span more than an order of magnitude, with the value chosen here being in the middle of the range. Because of the large uncertainty in this rate constant, laminar flame speed predictions using any particular set of diffusion coefficients recommended by various authors can be forced to predict the same flame speed simply by adjusting the value of this single rate constant.

RESULTS AND DISCUSSION

The mechanism updated as described above was compared against a wide range of experimental data, including laminar flame speed, shock tube ignition delay time, and the species profiles in VPFR, shock tube, and burner-stabilized flame studies. The SENKIN code [40] was used to simulate experimental conditions in a shock tube and flow reactor. The PREMIX code [41] was used for flame calculations. We used the standard CHEMKIN transport package [42] with multicomponent formulation and Soret effects included. A minimum of 1000 grid points was imposed in the PREMIX calculation for a fully converged flame speed value. Representative test results are shown in Figs. 7–18.

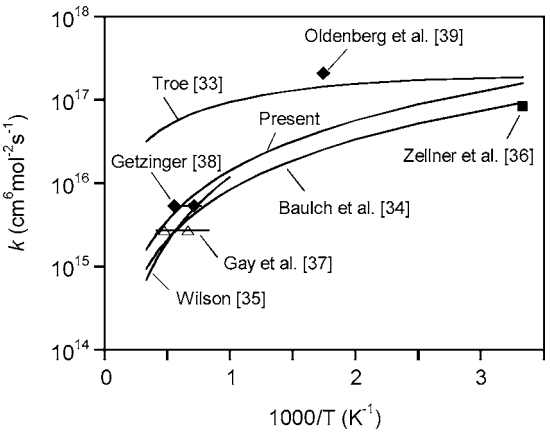

Figure 6 Rate constant of H + OH + M → H_2O + M for M = Ar.

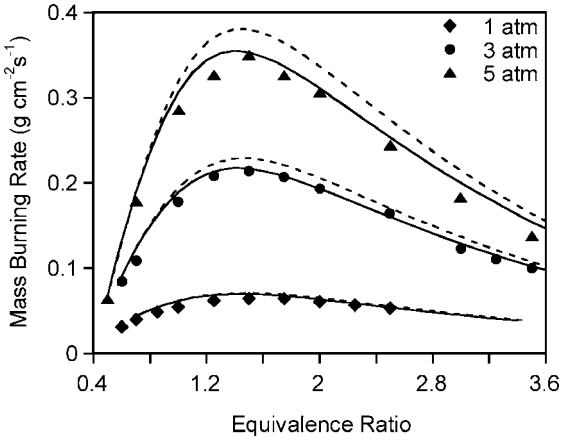

Figure 7 Laminar flame mass burning rate at 1, 3, and 5 atm for H_2/O_2/He mixture (O_2:He = 1:7). Symbols: experimental data [7]; solid lines: the present model; dashed lines: the model of Mueller et al. [1].

The comparisons in Figs. 7 and 8 show that the predictions of the present mechanism are in excellent agreement with the laminar flame speed measurements for H_2/O_2/He mixture at pressures ranging from 1 to 20 atm. The prediction of the laminar flame speed of

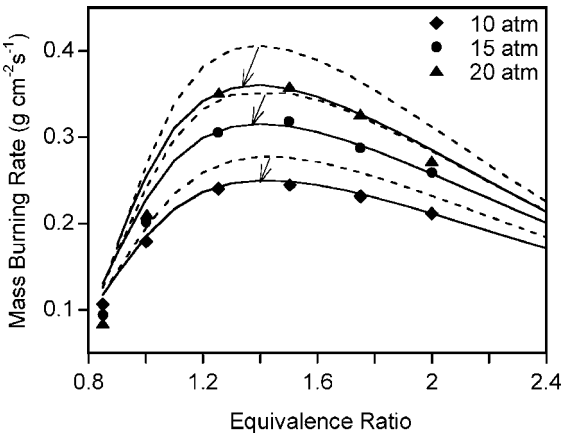

Figure 8 Laminar flame mass burning rate at 10, 15, and 20 atm for H_2/O_2/He mixture (O_2:He = 1:11.5). Symbols: experimental data [7]; solid lines: the present model; dashed lines: the model of Mueller et al. [1].

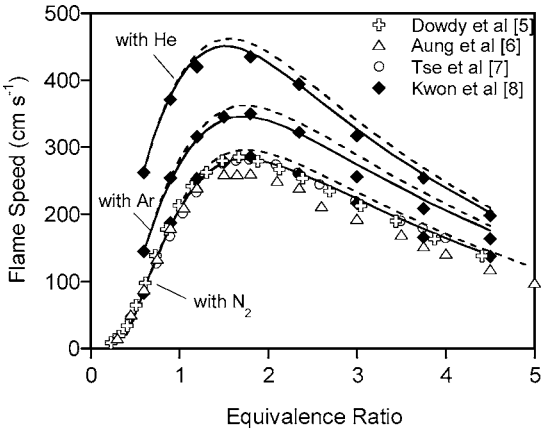

Figure 9 Laminar flame speed at 1 atm for H_2/O_2 diluted with N_2, Ar, or He. (O_2:N_2 = O_2:Ar = O_2:He = 1:3.76). Symbols: experimental data [5–8]; solid lines: the present model; dashed lines: the model of Mueller et al. [1].

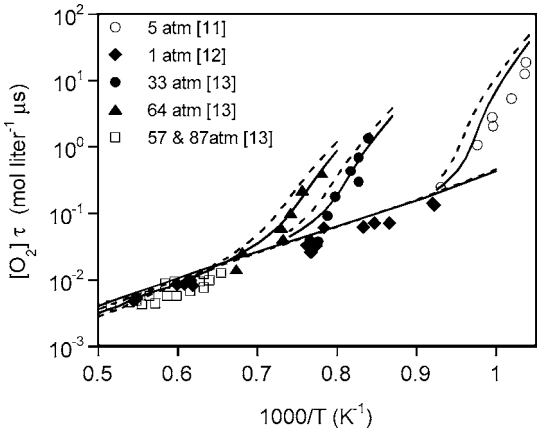

Figure 11 Ignition delay of H_2/O_2/Ar mixtures in shock tubes. Initial conditions: $H_2 = 8.0\%$, $O_2 = 2.0\%$ at 5 atm [11]; $H_2 = 1.0\%$, $O_2 = 2.0\%$ at 1 atm [12]; $H_2 = 2.0\%$, $O_2 = 1.0\%$ at 33, 57, 64, and 87 atm [13]. Symbols: experimental data [11–13]; solid lines: the present model; dashed lines: Mueller et al. [1]. Ignition delay time for the cases of Ref. [11] is defined by the maximum of OH concentration; for Ref. [12], as the time when OH concentration reaches 1×10^{-6} mol/L; and for Ref. [13], by the maximum of $\frac{d[OH]}{dt}$.

H_2/O_2 system diluted by N_2, Ar, or He at 1 atm is presented in Fig. 9.

Predictions also compare very well with shock tube ignition delay data, as is demonstrated with representative cases in Figs. 10–12. Figure 13 shows the reaction time when the OH mole fraction under shock tube conditions reaches a specific fraction of the equilibrium value. Figures 14 and 15 show the time history of the H and OH mole fraction in shock tube experiments. Clearly, the current mechanism agrees with the experimental measurements very well.

The original Mueller et al. mechanism was validated against 16 VPFR experiments [1]. Excellent agreement of the model predictions with the experimental measurement was demonstrated in Ref. [1]. The current mechanism was verified against all of these VPFR cases, and agrees with the experiments as well as the predictions using the original mechanism. Representative results are shown in Figs. 16 and 17. Time shift is used to compare the model predictions with the experimental measurement by shifting the simulated values along the time axis to match the 50% fuel consumption point.

The comparison of model predictions with species profiles measured in burner-stabilized flame [43] is

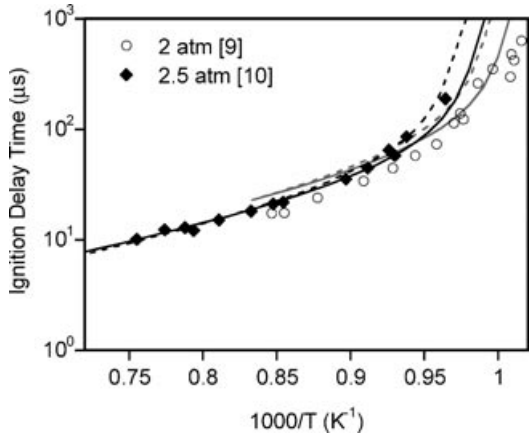

Figure 10 Ignition delay time of $H_2/O_2/N_2$ mixture at 2 atm or 2.5 atm ($H_2 = 29.6\%$, $O_2 = 14.8\%$). Symbols: experimental data [9,10]; solid lines: the present model; dashed lines: the model of Mueller et al. [1]. Ignition delay time is defined by a rapid increase in the pressure.

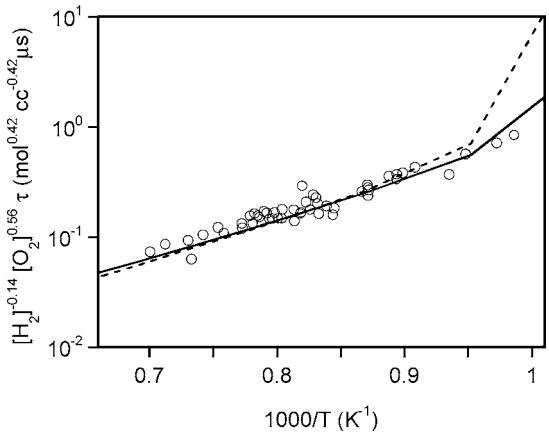

Figure 12 Ignition delay of H_2/O_2/Ar mixture at 2 atm ($H_2 = 6.7\%$, $O_2 = 3.3\%$). Symbols: experimental data [14]; solid lines: the present model; dashed lines: the model of Mueller et al. [1]. Ignition delay time is defined by a rapid rise of pressure.

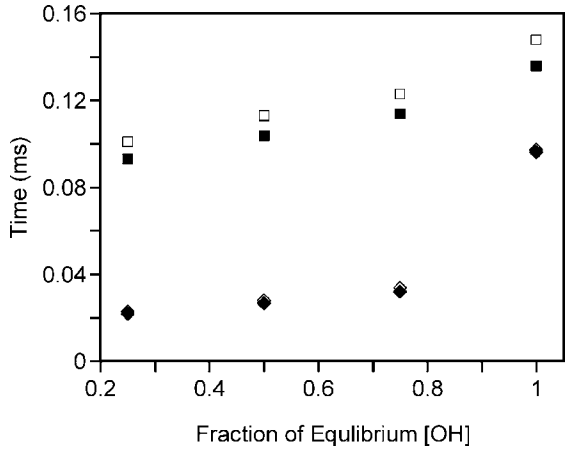

Figure 13 Reaction time in a shock tube when OH mole fraction reaches 0.25, 0.5, 0.75, and 0.99 times the equilibrium value, respectively. Initial conditions: $H_2 = 5.0\%$, $O_2 = 0.493\%$ with balance Ar at 0.675 atm and 1980 K (for squares); $H_2 = 1.10\%$, $O_2 = 0.208\%$ with balance Ar at 1.98 atm and 2898 K (for diamonds). Open symbols represent experimental data [25], and solid symbols the present mechanism.

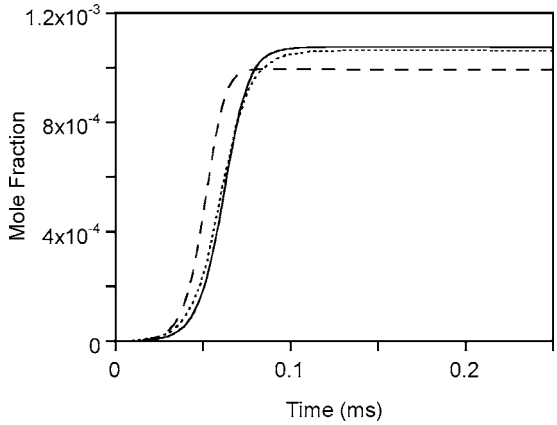

Figure 15 Time history of OH mole fraction in a shock tube. Initial conditions: $H_2 = 4002$ ppm, $O_2 = 3999$ ppm with balance Ar at 1.075 atm and 2590 K. Dotted line: experimental data [23]; solid line: the present model; dashed line: the model of Mueller et al. [1].

shown in Fig. 18. The experimental flame-temperature profile was used in the PREMIX calculation. Clearly, the predictions of the present mechanism and Mueller et al. [1] are almost the same and yield reasonably good level of agreement with the experiments, typical for premixed flame modeling [53].

CONCLUSION

The detailed H_2/O_2 reaction mechanism of Mueller et al. [1] has been updated using recently published rate constants of the reactions (R1) and (R2), and the thermodynamic data of OH. An important constraint on combinations of reactions (R1) and (R2) is provided by the ratio of these reactions in the temperature range 800–900 K. Above and below this temperature range, one or the other of these reactions becomes significantly less important, and determining their ratio at other temperatures is subject to higher uncertainties. Analyses also show that reaction (R3) is of significance to observations in the case of high-pressure flame propagation. The present uncertainties in experimental determinations, third-body effects, and theory are so large that within the bounded range the rate can be varied such that high pressure laminar flame speed data

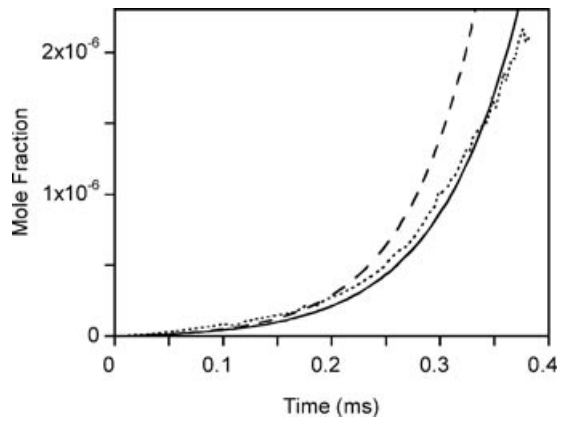

Figure 14 Time history of H mole fraction in a shock tube. Initial conditions: $H_2 = 0.99\%$, $O_2 = 0.10\%$ with balance Ar at 0.79 atm and 1700 K. Dotted line: experimental data [25]; solid line: the present model; dashed line: the model of Mueller et al. [1].

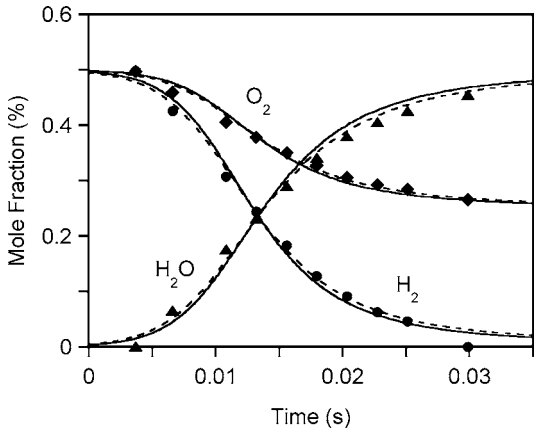

Figure 16 Reaction profiles of $H_2/O_2/N_2$ mixture in a flow reactor. Initial conditions: $H_2 = 0.50\%$, $O_2 = 0.50\%$ with balance N_2 at 0.3 atm and 880 K. Symbols: experimental data [1]; solid lines: the present model; dashed lines: the model of Mueller et al. [1].

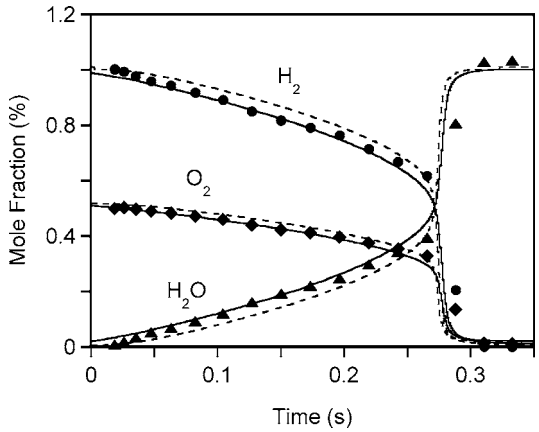

Figure 17 Reaction profiles of $H_2/O_2/N_2$ mixture in a flow reactor. Initial conditions: $H_2 = 1.01\%$, $O_2 = 0.52\%$ with balance N_2 at 3.4 atm and 933 K. Symbols: experimental data [1]; solid lines: the present model; dashed lines: the model of Mueller et al. [1].

can be modeled as satisfactorily by any proposed set of transport properties. Thus hydrogen–oxygen flame speed experiments cannot at present resolve whether sources of disparity are the modeling of transport properties, (R3), or experiment. Here, we modified the rate constant of reaction (R3) to achieve flame propagation

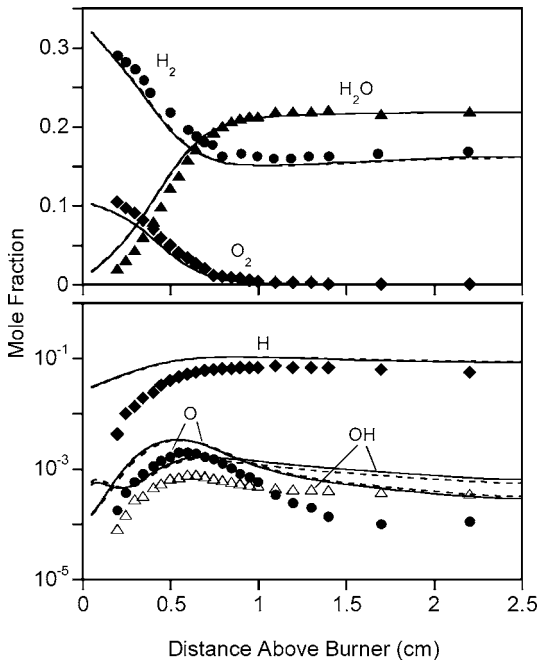

Figure 18 Species profiles of $H_2/O_2/Ar$ mixture in burner-stabilized flame. Initial conditions: $H_2 = 39.7\%$, $O_2 = 10.3\%$ with balance Ar at 4.75 kPa. Symbols: experimental data [43]; solid lines: the present model; dashed lines: the model of Mueller et al. [1].

model performance using the transport properties from the CHEMKIN transport package [42].

The present mechanism is compared against a wide range of experimental conditions (298–3000 K, 0.3–87 atm, $\phi = 0.25$–5.0) found in laminar premixed flames, shock tubes, and flow reactors. Very good agreement of the model predictions with the experimental measurement demonstrates that the updated comprehensive mechanism has excellent predictive capabilities for different experimental systems. The current mechanism in an electronic form compatible with CHEMKIN II is available from the authors on request.

BIBLIOGRAPHY

1. Mueller, M. A.; Yetter, R. A.; Dryer, F. L. Int J Chem Kinet 1999, 31, 113.
2. Yetter, R. A.; Dryer, F. L.; Rabitz, H. Combust Sci Tech 1991, 79, 97.
3. Westbrook, C. K.; Dryer, F. L. Combust Sci Tech 1979, 20, 125.
4. Westbrook, C. K., Dryer, F. L. In 18th Symposium (International) on Combustion, The Combustion Institute, Pittsburgh, PA, 1981; p. 749.
5. Dowdy, D. R.; Smith, D. B.; Taylor, S. C. In 23th Symposium (International) on Combustion, The Combustion Institute, Pittsburgh, PA, 1990; p. 325.
6. Aung, K. T.; Hassan, M. I.; Faeth, G. M. Combust Flame 1997, 109, 1.
7. Tse, S. D.; Zhu, D. L.; Law, C. K. In Proceedings of the Combustion Institute, The Combustion Institute, Pittsburgh, PA, 2000; pp. 28, 1793.
8. Kwon, O. C.; Faeth, G. M. Combust Flame 2001, 124, 590.
9. Slack, M. W. Combust Flame 1977, 28, 241.
10. Bhaskaran, K. A.; Gupta, M. C. Just, Th. Combust Flame 1973, 21, 45.
11. Skinner, G. B.; Ringrose, G. H. J Chem Phys 1965, 42, 2190.
12. Schott, G. L.; Kinsey, J. L. J Chem Phys 1958, 29, 1177.
13. Petersen, E. L.; Davidson, D. F.; Rohrig, M; Hanson, R. K. AIAA Paper 95-3113, 31st AIAA/ASME/SAE/ASEE Joint Propulsion Conference and Exhibit, San Diego, 1995.
14. Cheng, R. K.; Oppenheim, A. K. Combust Flame 1984, 58, 125.
15. Curran, H. J., personal communication, June 2003.
16. Hessler, J. P. J Phys Chem A 1998, 102, 4517.
17. Troe, J. In Proceedings of the Combustion Institute, The Combustion Institute, Pittsburgh, PA, 2000; pp. 28, 1463.
18. Bates, R. W.; Golden, D. M.; Hanson, R. K.; Bowman, C. T. Phys Chem Chem Phys 2001, 3, 2337.
19. Michael, J. V.; Su, M. C.; Sutherland, J. W.; Carroll, J. J.; Wagner, A. F. J Phys Chem A 2002, 106, 5297.

20. Ashman, P. J.; Haynes, B. S. In 27th Symposium (International) on Combustion, The Combustion Institute, Pittsburgh, PA, 1998; p. 185.
21. Mueller M. A.; Yetter, R. A.; Dryer, F. L. In 27th Symposium (International) on Combustion, The Combustion Institute, Pittsburgh, PA, 1998; p. 177.
22. Ruscic, B.; Wagner, A. F.; Harding, L. B.; Asher, R. L.; Feller, D.; Dixon, D. A.; Peterson, K. A.; Song, Y.; Qian, X.; Ng, C.; Liu, J. Chen, W.; Schwenke, D. W. J Phys Chem A 2002, 106, 2727.
23. Herbon, J. T.; Hanson, R. K.; Golden, D. M.; Bowman, C. T. In Proceedings of the Combustion Institute, The Combustion Institute, Pittsburgh, PA, 2002; pp. 29, 1201.
24. Pirraglia, A. N.; Michael, J. V.; Sutherland, J. W.; Klemm, R. B. J Phys Chem 1989, 93, 282.
25. Masten, D. A.; Hanson, R. K.; Bowman, C. T. J Phys Chem 1990, 94, 7119.
26. Du, H.; Hessler, J. P. J Chem Phys 1992, 96, 1077.
27. Ryu, S. O.; Hwang, S. M.; Rabinowitz, M. J. J Phys Chem 1995, 99, 13984.
28. Yu, C. L.; Frenklach, M.; Masten, D. A.; Hanson, R. K.; Bowman, C. T. J Phys Chem 1994, 98, 4770.
29. Yuan, T.; Wang, C.; Yu, C.-L.; Frenklach, M.; Rabinowitz, M. J. J Phys Chem 1991, 95, 1258.
30. Gilbert, R. G.; Luther, K.; Troe, J. Ber Bunsenges Phys Chem 1983, 87, 169.
31. Mueller, M. A. Ph.D. thesis, Princeton University, Princeton, NJ, 2000.
32. Scire, J. J. Jr.; Dryer, F. L.; Yetter, R. A. Int J Chem Kinet 2001, 33, 784.
33. Troe, J. J Phys Chem 1979, 83, 114.
34. Baulch, D. L.; Cobos, C. J.; Cox, R. A.; Esser, C.; Frank, P.; Just, Th.; Kerr, J. A.; Pilling, M. J.; Troe, J.; Walker, R. W.; Warnatz, J. J Phys Chem Ref Data 1992, 21, 411.
35. Wilson, W. E. Jr. J Phys Chem Ref Data 1972, 1, 535.
36. Zellner, R.; Erler, K.; Field, D. In 16th Symposium (International) on Combustion, The Combustion Institute, Pittsburgh, PA, 1977; p. 939.
37. Gay, A.; Pratt, N. H. In Proceedings of the International Symposium Shock Tubes Waves, 1971; 8, p. 39.
38. Getzinger, R. W. In 11th Symposium (International) on Combustion, The Combustion Institute, Pittsburgh, PA 1967, 117.
39. Oldenberg, O.; Rieke, F. F. J Chem Phys 1939, 7, 485.
40. Lutz, A. E.; Kee, R. J.; Miller, J. A. Report SAND-87-8248; Sandia National Laboratories: Albuquerque, NM, 1988.
41. Kee, R. J.; Grcar, J. F.; Smooke, M. D.; Miller, J. A. Report SAND85-8240; Sandia National Laboratories: Albuquerque, NM, 1985.
42. Kee, R. J.; Dixon-Lewis, G.; Warnatz, J.; Coltrin, M. E.; Miller, J. A. Report SAND86-8246; Sandia National Laboratories: Albuquerque, NM, 1986.
43. Vandooren, J.; Bian, J. In 23rd Symposium (International) on Combustion, The Combustion Institute, Pittsburgh, PA, 1990; p. 341.
44. Sutherland, J. W.; Michael, J. V.; Pirraglia, A. N.; Nesbitt, F. L.; Klemm R. B. In 21st Symposium (International) on Combustion, The Combustion Institute, Pittsburgh, PA, 1986; p. 929.
45. Michael, J. V.; Sutherland, J. W. J Phys Chem 1988, 92, 3853.
46. Sutherland, J. W.; Patterson, P. M.; Klemm, R. B. In 23rd Symposium (International) on Combustion, The Combustion Institute, Pittsburgh, PA, 1990; p. 51.
47. Tsang, W.; Hampson, R. F. J Phys Chem Ref Data 1986, 15, 1087.
48. Cobos, C. J.; Hippler, H.; Troe, J. J Phys Chem 1985, 89, 342.
49. Hippler, H.; Troe, J.; Willner, J. J Chem Phys 1990, 93, 1755.
50. Warnatz, J. In Combustion Chemistry; Gardiner, W. C. (Ed.); Springer-Verlag: New York, 1985.
51. Brouwer, L.; Cobos, C. J.; Troe, J.; Dubal, H. R.; Crim, F. F. J Chem Phys 1985, 86, 6171.
52. Hippler, H.; Troe, J. Chem Phys Lett 1992, 192, 333.
53. Vandooren, J.; Van Tiggelen, P. J. Combust Flame 1997, 109, 647.
54. Ruscic, B. In 25th Annual Combustion Research Conference, Arlie Conference Center, Warrenton, VA, June 2004; p. 253; http://cmcs.org.